Characterization Of Silver Nanoparticles Using Aqueous Leaf Extract Of Murrayakoenigii And Its Antioxidant Potential

Ashok Kumar Tripathi[1], Jhansee Mishra[2*]

[1]Institute of Pharmacy V.B.S. Purvanchal University, Jaunpur, Uttar Pradesh, India
[2*]Assistant Professor, Institute of Pharmacy V.B.S. Purvanchal University, Jaunpur, Uttarpradesh, India
Email: alokjina@gmail.com Mob:9648349477

***Corresponding Author:** Dr. Jhansee Mishra
*Assistant Professor, Institute of Pharmacy V.B.S. Purvanchal University, Jaunpur, Uttarpradesh, India
Email: alokjina@gmail.com Mob:9648349477

Abstract
The use of microbes, enzymes, or plant extracts in biological methods to synthesize nanoparticles has been proposed as a potentially environmentally acceptable substitute for chemical and physical procedures that need the use of hazardous reducing agents. In the current study, MurrayaKoenigii leaf extract was used to create silver nanoparticles (AgNPs) using a green method. Fourier Transform Infrared (FTIR), UV-visible (UV-vis), and scanning electron microscopy (SEM) were used to analyze the produced AgNPs. The total phenolic content (TPC) of the produced AgNPs, the total reductive potential, and the DPPH radical scavenging experiment were used to assess the antioxidant activity. The produced silver nanoparticles had a size range of 50–70 nm and a maximum UV–vis absorbance of 480 nm, according to SEM examination. The synthesized AgNPs exhibited a dose-dependent increase in DPPH radical scavenging activity, reducing power, and total phenolic and total flavonoid contents when compared to the standard reference, ascorbic acid. This outcome demonstrated that MurrayaKoenigii is a promising biomaterial with the ability to synthesize AgNPs and be used for their antioxidant properties.

Keywords: DPPH radical scavenging activity, antioxidant activity, silver nanoparticles, and free radicals.

1. INTRODUCTION

In living systems that are oxygen-dependent (aerobic), free radicals are essential. They contribute to vital cellular functions including respiration, but they also play a role in the onset of aging and illness [1, 2]. Because their free electrons are continually trying to form covalent partnerships with other electrons, free radicals are unstable molecules with free unpaired electrons. This makes them extremely reactive. The free radicals in this process strip other molecules of their electrons. It can harm components including proteins, carbohydrates, lipids, and nucleic acids in addition to altering cell regulation [3, 4]. Free radicals can originate from a variety of places both inside and outside of cells. Free radicals are created during regular metabolic activities in aerobic organisms [5]. The two main sources are cell respiration in the mitochondrial membrane and electron transport in the plasma membrane. Due to the ability of free radicals like superoxide to evade the electron transport chain, mitochondria are the primary source of oxidative damage [6, 7]. Cells have developed an intracellular antioxidant mechanism to guard against intracellular damage caused by free radicals.

By preventing, postponing, or impeding the oxidation of the biomolecules, antioxidants regulate oxidative processes [8, 9]. Certain components of the main antioxidant enzymes shelter and protect proteins [10, 11]. Antioxidants that are not enzymatic in nature can also counteract free radicals. Examples of these include fat-soluble nutrients like vitamin E and β-carotene and water-soluble nutrients like vitamin C and glutathione [8, 12, 13]. According to recent reports, synthetic antioxidants such butylated hydroxyl toluene (BHT) and butylated hydroxyl anisole (BHA) are detrimental to human health [14, 15]. As a result, there has been a rise in the hunt for safe, natural chemicals with antioxidant activity that are also beneficial in recent years. Because of the significant advantages of their biomedical applications, such as drug delivery, medical imaging, disease diagnosis, cancer treatment, infectious disease treatment, treatment of neurodegenerative disorders, including Parkinson disease [22], and so forth, nanomaterials have recently begun to play a fundamental role in human life and health [16].

Furthermore, some nanomaterials' significant antioxidant properties are creating interesting opportunities for the development of novel regimens with improved and focused activities. For instance, because of their effective redox-active radical-scavenging abilities, gold, silver, and selenium nanoparticles have been demonstrated to have the capacity to lessen oxidative stress [23, 24].

2 MATERIALS AND METHODS

2.1 Preparation of Leaf Extract

Pharmacy Department of Veer Bahadur Singh Purvanchal University provided the fresh MurrayaKoenigii leaves that were harvested and properly cleansed with double-distilled water. From these, plant materials were taken out. It was combined with 150 milliliters of distilled water and 10 grams of powdered leaves. To extract the components of the leaves, the solution were heated to 100^0C for two minutes, cooled to room temperature, and then filtered using Whatman 1 filterpaper. The extracted solution was stored at 4 degrees Celsius.

2.2 Silver Nanoparticle Synthesis

To make silver nanoparticles, we employed the MurrayaKoenigii aqueous leaf extract that was prepared in the earlier step. This required adding 10 mL of leaf extract and boiling 90 mL of a 1 mM aqueous silver nitrate solution for three hours at 80 °C while stirring constantly. The first sign of the AgNPs' development was the color change from yellow to dark brown. The green-produced nanoparticles were separated using centrifugation for 20 minutes at 15,000 × g. This process was repeated three times in order to eliminate the free silver associated with Cp-AgNPs. The last green-synthesised silver nanoparticles, or Cp-AgNPs, were freeze-dried and stored at 4 °C until they were required once more.

2.3 Characterization of Green Synthesized Silver Nanoparticles

2.3.1 UV-Vis Spectroscopy

In order to monitor the production of silver nanoparticles, the optical density of the reaction mixture was measured at different time intervals using Milli Q water as a blank using a Shimadzu UV-1800 double beam UV–Vis spectrophotometer. The absorbance of the reaction mixture was measured between 300 and 700 nm.

2.3.2 SEM Analysis of Silver Nanoparticles

Scanning electron microscopy (SEM) analyses were performed on an EVOSEM MA 15/18 that was equipped with an EDS instrument. A very little amount of the sample was dropped onto a copper grid to create a thin film of the material. To determine whether elemental silver was present in AgNPs, the size and shape of the nanoparticles were investigated using a scanning electron microscope (Nova Nano SEM 450, USA).

2.3.3 TEM Analysis

The produced AgNPs colloidal solution is centrifuged at 10,000 rpm for 15 minutes at 25 °C to remove the non-covalently attached molecules from their surfaces in order to prepare the sample for analysis using transmission electron microscopy (TEM; Tecnai G2-F20 TWIN, FEI USA). It was further sonicated to ensure that the nanoparticles were evenly distributed. A copper grid was covered with a few droplets of the solution, which were then equally distributed across the grid to form a thin film. The grid was dried in a hot air oven (NSW-India-143) for 120 minutes at 50 °C. The size of the nanoparticles was also investigated at different magnifications. (25)

2.3.4 XRD

The X-ray diffraction pattern (XRD) of AgNPs was investigated using an X-ray diffractometer (Rigaku Minifex 600) equipped with a Cu Kα radiation source and a nickel monochromator filter in the 2θ range of 20°–80° at a scanning rate of $2° \text{ min}^{-1}$. For this investigation, a glass microscope slide containing a nanoparticle solution was utilized. The procedure was repeated in order to form a layer on the glass slide. In a hot air oven, the glass slide was fully dried at 60 °C. The dehydrated AgNPs were discarded in order to conduct more research. The average particle size of the AgNPs was calculated using the Debye-Scherer equation. where λ is the wavelength of the X-ray source (0.1541), which is used in XRD; β is the diffraction angle; and together these values indicate the full width at the half maximum of the diffraction peak. where D is the average crystallite domain size, which is perpendicular to the reflecting planes; K is the Scherer's constant, with a value between 0.9 and 1. Selected area electron diffraction (SEAD) was used to confirm the crystalline nature of AgNPs.

2.3.5 Analysis of Infrared Fourier Transform Spectroscopy (FT IR)

The surface structure of the silver nanoparticle was characterized in the wavelength range of 4000–400 cm−1 by recording the Fourier transform infrared (FTIR) spectra of the dried extract and nanoparticle using an FTIR spectrophotometer (Bruker, Germany).

2.4 In Vitro DPPH Assay

The DPPH scavenging activity of plant extracts against stable 2, 2 diphenyl 2 picryl hydroxyl hydrate (DPPH) was determined using a slightly modified Brand-W method. In the presence of an antioxidant, DPPH can contribute hydrogen and undergo reduction. The hue shift (from deep violet to pale yellow) was detected at 517 nm using a BMG Fluostar (GERMANY). The percentage inhibition data was assessed using BMG's (Germany) MARS program. A daily fresh solution of DPPH in methanol 6 × 10-5 M was prepared prior to UV measurements. Three milliliters of this solution were mixed with different plant extracts at a concentration of 100 micrograms/ml and a herbal preparation. The absorbance decreased after fifteen minutes at room temperature and darkness for the samples. (26) The ratio of [(Control absorbance - sample absorbance)/control absorbance] × 100 is the proportion of DPPH free radical scavenging activity.

2.5 Reduced Glutathione

With GSH and a chromophore present, the Reduced Glutathione (GSH) Assay Kit uses an enzymatic cycling approach. The reduction of the chromophore yields a stable product, which may be kinetically observed by measuring the absorbance at 450 nm (A450). As a result, there is a direct correlation between the sample's GSH level and absorbance. The kit is very sensitive and specific since GSSG does not interact with the test. 5. The kit contains sulfosalicylic acid (SSA) to protect the endogenous GSH content in the samples. The assay is simple to use and reliable, and it can accurately detect reduced glutathione (GSH) in a 100 L reaction as little as 50 pmol/well (SSA serves as an antioxidant and deproteinizing agent). To summarize, 10ul of substrate mix A is mixed with 1ul of enzyme mix B, 2ul of enzyme mix C, 2ul of substrate mix C, and 55ul of GSH assay buffer (Table 2). Then, at 450 nm, the OD is calculated. To facilitate computations, the GSH from the standard curve/ (reaction volume added to sample X sample concentration in mg protein/ml) X sample dilution factor is given in nmol/mg (Fig. 7).

2.6 Lipid Peroxidase TBARS (MDA) Assay

Each well is filled with 200 µL of the sample and 600 µL of the TBA reagent. At 95°C, incubated for 60 minutes then it was cooled down to room temperature for 10 minutes using an ice bath. 200 µL of the reaction mixture, which contains the MDA-TBA adduct, was transferred into a 96-well microplate for analysis. The absorbance was determined immediately for a colorimetric experiment using a microplate reader set to OD 532 nm.

3. RESULTS

3.1 Enhancement of the UV-Vis Spectroscopy Application of Silver Nanoparticle Biosynthesis

After adding the green leaf extract and letting the mixture sit in the light at room temperature, the reaction mixture's color changed from green to a colorless silver nitrate solution. As seen in Fig. 1a, the color of the reaction mixture turned brown. The maximum absorbance of the reaction mixture was found at 460 nm (Fig. 1b). The silver surface plasmon resonance (SPR) peak is located here. The biosynthesis of silver nanoparticles was confirmed. To create high-quality nanoparticles, a number of factors were evaluated, such as the extract amount (0.1–2%), silver nitrate (0.5–5 mM), and the duration of light exposure (5–30 min).

3.2 SEM Assessment

Using scanning electron microscopy, a well-defined, spherical, aggregation-free silver nanoparticle (Fig. 2) was discovered. With the use of a scanning electron microscope, the size and shape of the nanoparticles were examined (Nova Nano SEM 450, USA).

3.3 TEM Assessment

TEM images of the generated silver nanoparticles were captured at different magnifications. The findings show that the nearly spherical green nanoparticles made via biosynthesis have a size range of 10 to 50 nm (Fig. 3).

3.4 Schematic for XRD

The polycrystalline nature of AgNPs was confirmed by the XRD pattern analysis (Fig. 6). The XRD spectrum showed four prominent diffraction peaks at 2θ values of 38.18°, 44.25°, 64.25°, and 77.40°. These numbers matched values indexed at the (111), (200), (220), and (311) lattice planes. Bragg's reflections of the face-centered cubic (FCC) structure of metallic silver. The XRD examination confirmed the identity of the resultant particles as silver nanoparticles. The broad and noticeable spectrum peaks of silver nanoparticles reveal their small particle size and crystalline structure.

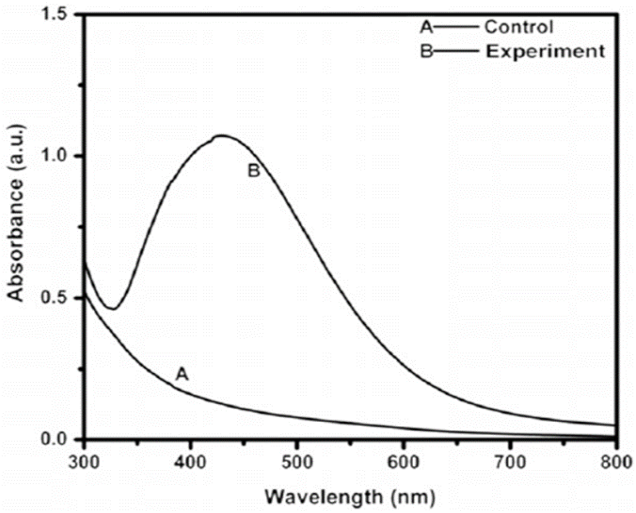

Fig.1 Green synthesis of silver nanoparticles: After adding leaf extract to the silver nitrate solution, the reaction mixture's colour changed from yellowish green to brown. The biogenesis of silver nanoparticles, with λ max = 480 nm, was confirmed by the UV-Vis spectrum (online colour figure).

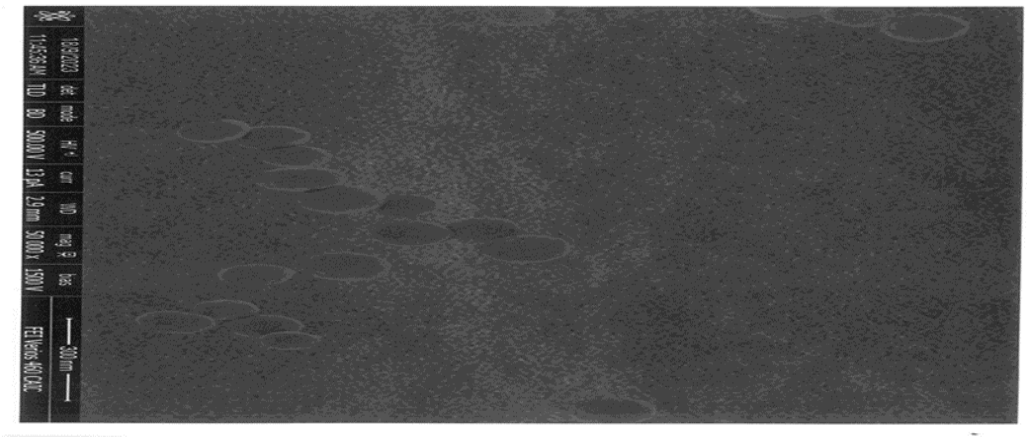

Fig. 2 SEM study of biosynthesized silver nanoparticles.

MurrayaKoenigii AgNPs, produced nanoparticles are shown in

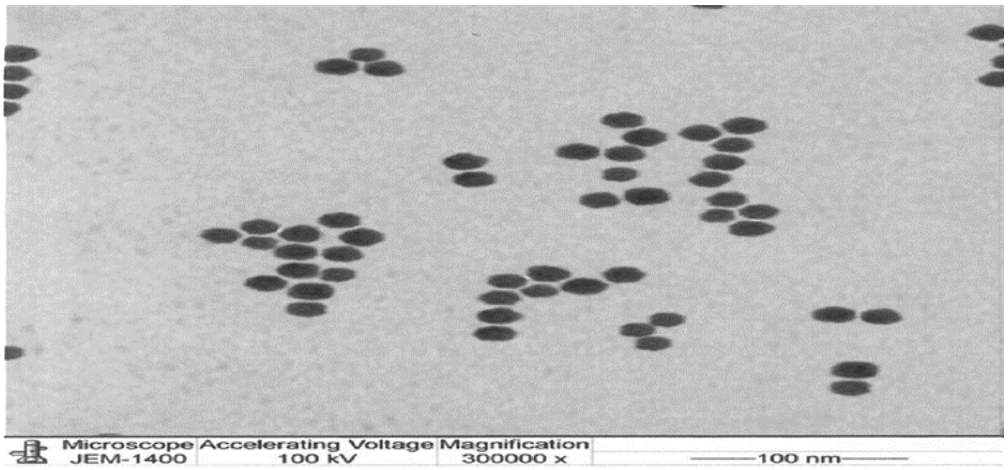

Fig. 3: Topographical view of MurrayaKoenigii AgNPs colloid silver nanoparticle from TEM examination a–c at varying magnifications

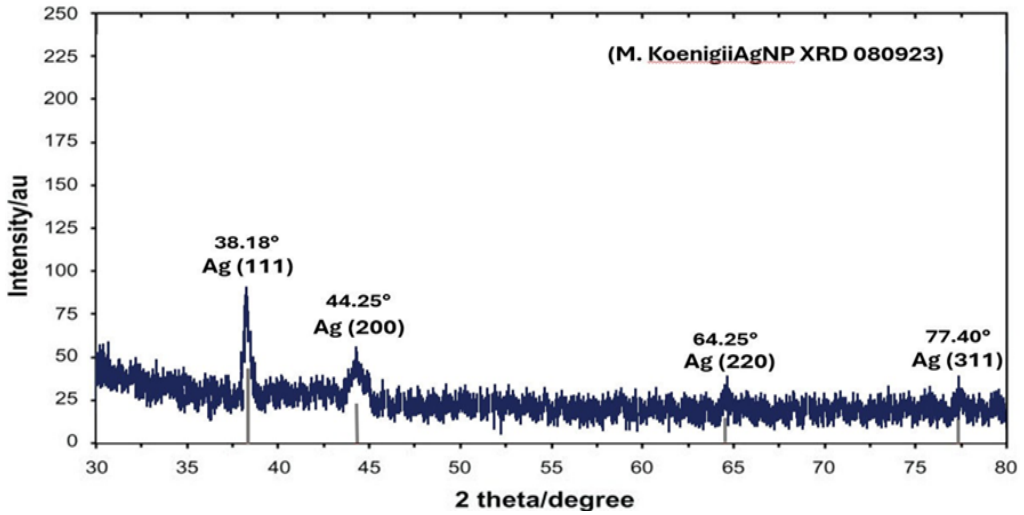

Fig 4: X-ray diffraction pattern of silver nanoparticles made with MurrayaKoenigii AgNPs aqueous leaf extract

3.5 FTIR Examination

The FTIR spectra of the leaf extract and biosynthesised silver nanoparticles were shown in figure 5. The leaf extract FTIR spectrum (Fig. 5) showed peaks at 3857.44, 3721.96, 3507.28, 3454.89, 3394.96, 3285.57, 2920.82, 2855.61, 2382.04, 2312.32, 2103.68, 1557.39,1420.01,1050.33,677.34, 610.02, and 529.64 cm-1. The leaf extract's absorption peaks in the 4000–3000 cm−1 range (3857.44, 3721.96, 3507.28, 3454.89, 3394.96, and 3285.57 cm−1) suggested the existence of an O–H stretching hydroxyl functional group, either in the free state or in strong hydrogen bonding. These peaks indicate the presence of phytoconstituents such flavonoids, polyphenols, and tannins. In the 3000–2000 cm−1 wavelength range, the following peaks (2920.82, 2855.61, 2382.04, 2312.32, and 2103.68cm−1) offer information about the presence of C–

H stretching alkanes. The highest wave numbers in the 2000–1000 cm−1 range were 1724.28, 1557.39, 1420.01, and 1050.33 cm−1. These results show that C=O, C=N, C=C, O–H, and C–H stretching exist, suggesting the potential presence of glycosides, tannins, and triterpenes. Within the 1000–500 cm−1 range, the peaks at 677.34, 610.02, and 529.64 cm-1 indicate the presence of O–C and alkyl halide (C–X) stretching. It demonstrates how acidic components and meta-aromatic hydrocarbons can coexist. The polyphenolic components present in the extract, which correspond to the H-bond, OH stretch, and C-H stretch, may be important in the reduction and capping of silver ions, as suggested by the absence of peaks in the FTIR of the nanoparticles.

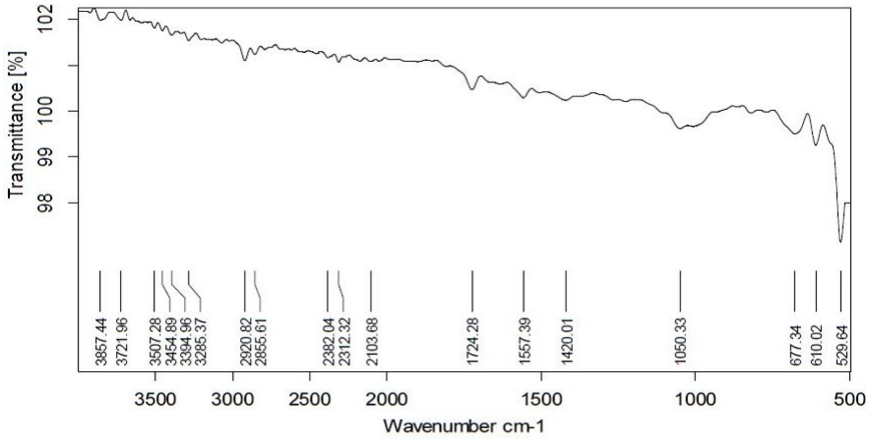

Wavenumber	Abs. intensity	Rel. intensity	Width	Found if threshold <	Shoulder
3857.4383	1.020	0.002	69.2703	3.494142	0
3721.9556	1.020	0.002	47.7874	4.345758	0
3507.2813	1.018	0.001	26.2902	2.070275	0
3454.8853	1.018	0.001	25.3143	1.918700	0
3394.9577	1.017	0.001	3909.6901	1.628143	0
3285.3652	1.015	0.002	50.7039	3.044782	0
2920.8220	1.011	0.005	57.4560	6.735738	0
2855.6132	1.012	0.001	31.1602	2.621773	0
2382.0382	1.012	0.001	50.1395	1.518310	0
2312.3241	1.011	0.002	36.4657	3.120103	0
2103.6832	1.011	0.001	113.5237	1.584537	0
1724.2787	1.005	0.003	28.2899	5.891351	0
1557.3874	1.003	0.002	30.1627	3.863051	0
1420.0084	1.002	0.002	3255.8803	3.273543	0
1050.3331	0.996	0.006	185.4075	9.807104	0
677.3373	0.995	0.005	63.2120	8.623424	0
610.0214	0.993	0.005	21.8198	8.488056	0

Fig-5 FTIR Spectra *MurrayaKoenigii* Ag NPs

Table 1: In-vitro free radical scavenging activity of silver nanoparticle and leaf extract of M. Koenigii L. evaluated by DPPH method .percentage (mean±SE)

Name of sample	**Results (DPPH OD450)**
Uninduced Untreated	0.60 ± 0.02
Induced Untreated	1.23 ± 0.01
M. Koenigii Ext	1.32 ± 0.02
M. KoenigiiAgNPs	1.57 ± 0.02
Ascorbic acid	2.47 ± 0.03

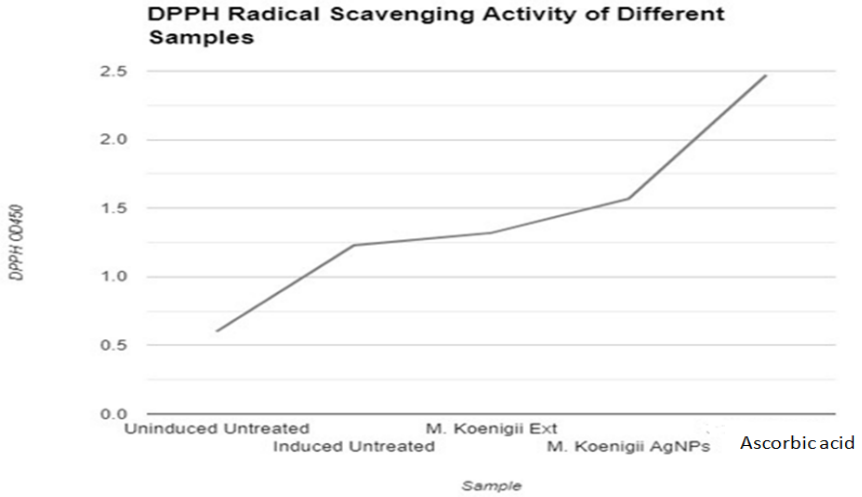

Fig-6: In-vitro free radical scavenging activity of silver nanoparticle and leaf extract of MurrayaKoenigii L. evaluated by DPPH method

Name of sample	Results (GSH OD 450)
Uninduced Untreated	1.49 ± 0.02
Induced Untreated	1.162 ± 0.01
M. Koenigii Ext	1.33 ± 0.01
M. KoenigiiAgNPs	1.32 ± 0.01
Gilbenclamide	1.48 ± 0.02

Table 2: Reduced Glutathione (GSH) Assay of silver nanoparticle and leaf extract of M. Koenigii L.percentage (mean±SE)

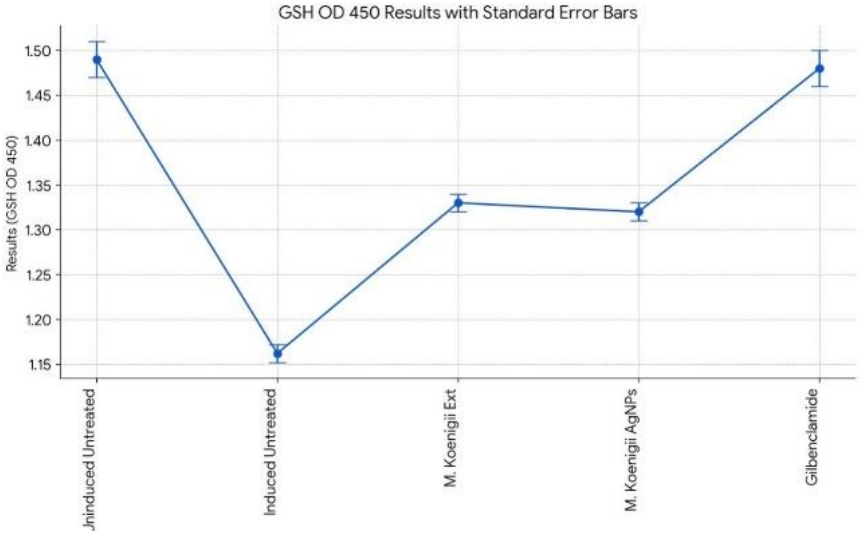

Figure 7: Reduced Glutathione (GSH) Assay of silver nanoparticle and leaf extract of M. Koenigii L.

Name of sample	Results (TBARS OD450)
Uninduced Untreated	0.92 ± 0.02
Induced Untreated	1.82 ± 0.02
M. KoenigiiExt	2.90 ± 1.2
M. KoenigiiAgNPs	1.40 ± 0.01
Gilbenclamide	0.87 ± 0.04

Table -3 Lipid Peroxidase assay TBARS (MDA) Assay of silver nanoparticle and leaf extract of M. Koenigii L.percentage (mean±SE)

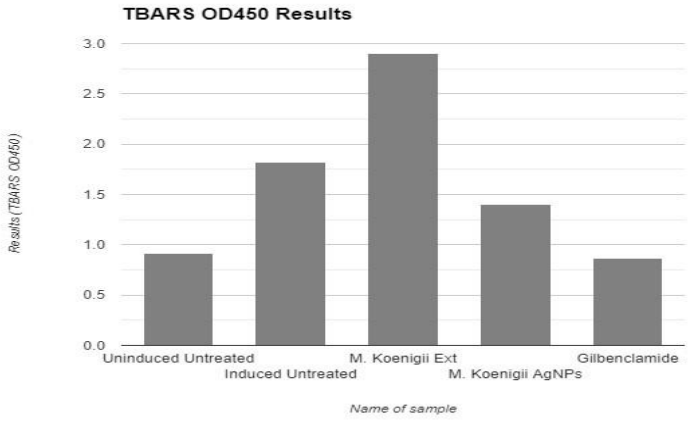

Fig-8 Lipid Peroxidase assay TBARS (MDA) Assay of silver nanoparticle and leaf extract of M. Koenigii L.

4- DISCUSSION:

The UV-Vis spectrum revealed that increasing the reaction time length led to a higher concentration of spherical silver nanoparticles forming, which produced a sharper, higher-intensity SPR band. The size of the generated nanoparticle is determined by the concentration of silver nitrate. The size of the particles increased with the concentration of silver nitrate [26]. Numerous techniques, including TEM, SEM, XRD, and FTIR analysis, were used to describe the AgNPs. The size and form of the nanoparticles were ascertained by TEM inspection [1]. Round-shaped biosynthesized silver nanoparticles were employed in this investigation. Similarly, it has been demonstrated that MurrayaKoenigii can produce spherical

nanoparticles. The manufacturing pattern of the nanoparticles, including whether they were made singly or in aggregates, was revealed by the SEM image. AgNPs' bioactivity and size showed a clear relationship. The XRD data suggests that the materials produced during biosynthesis are polycrystalline. The present study verified the well-crystalline nature of AgNPs. [27]FTIR analysis verified the possible teams responsible for both the reduction of silver ions and the capping of silver nanoparticles. The FTIR spectrum clearly shows that the material exhibits noticeable, selective absorptions in the infrared spectrum, based on the surface chemistry of the nanoparticle. Flavonoids, phenolics, and anthocyanins are examples of phytochemicals that have been of great interest as sources of natural antioxidants. It has been observed that plant components like fruits, seeds, grains, and green vegetables naturally contain antioxidants. A class of secondary plant phenols known as flavonoids has potent antioxidant qualities [28]. Since phenols are thought to be the primary oxidative components of plants, studies have found a relationship between total phenolics concentration and antioxidant capacity [29]. Phenols' primary source of antioxidant action is their redox characteristics, which are crucial for scavenging and neutralizing free radicals. According to the current study, the plant's high phenolic and flavonoid content may be the reason for the AgNPs' antioxidant action. These plant-based phenolics have a high potential for reduction and are potent antioxidants [30]. MurrayaKoenigii's capacity to reduce silver ions or create silver nanoparticles through reduction is probably brought about by the presence of electron-donating phenolic chemicals.

5. CONCLUSION

This study described the environmentally friendly, straightforward manufacture of silver nanoparticles utilizing MurrayaKoenigii leaf extract in aqueous form. FTIR tests confirmed that the leaf extract contains protein, carbohydrates, and phenolic chemicals, which may be responsible for the silver ion's bio-reduction and the stabilization of the silver nanoparticles. The biosynthesized silver nanoparticles derived from MurrayaKoenigii leaf extract demonstrated antioxidant activity by scavenging DPPH radicals, having a high phenolic and flavonoid content, and having the ability to undergo reduction. This study sheds light on the use of MurrayaKoenigii leaf as an excellent source of naturally occurring antioxidants and highlights its potential value as a medicinal agent for the prevention or treatment of disorders linked to oxidative stress.

References

1. Harrman D 1992 Role of free radicals in aging and diseases. Ann. N. Y. Acad. Sci.673 (1) pp 126-141.
2. Bagchi K and Puris S (1994) Free radical and antioxidants in health and disease. East. Mediterr. Health J. 4 pp 350-360.
3. Young I S and Woodside J V 2001 Antioxidants in health and disease. J. Clin. Pathol.54 (3) pp 176-186.
4. AK Dash, J Mishra, DK Dash : Antidiabetic activity and modulation of antioxidant status by Ocimum canum in streptozotocin-induced diabetic rats; European Scientific Journal, Volume,10,issue-6(2014)
5. Mohammed AA and Ibrahim AA 2004 Pathological roles of reactive oxygen species and their deference mechanism. Saudi Pharmaceut. J. 12 (6) pp 1-18.
6. Shigenaga M K, Hager T M and Ames B N 1994 Oxidative damage and mithochondria decay in aging. Proc. Natl. Acad. Sci. USA 91 (23) pp 10771-10778.
7. J Mishra, AK Dash, S Kumar :Hundred problems, one solution asparagus racemosus World Journal of Pharmaceutical Research, Volume 3,Issue-1,201-211(2013)Sies H 1997 Oxidative stress oxidants and antioxidants. Exp. Physiol. 82 (2): 291-295.
8. Kumar S 2011 Free radicals and antioxidants: Human and food system. Adv. Appl. Sci. Res. 2 (1) pp 129-135.
9. J Mishra, AK Dash, DK Dash - Nature's Drug Store: The Free Tree of India; World Journal of Pharmacy and Pharmaceutical,volume-2, 4778-98(2013)
10. Harris ED 1992 Copper as a cofactor and regulation of copper, zinc superoxide dismutase. J. Nutr. 122 (suppl_3) pp 636-640.
11. Trombino S, Serini S, Di-Nicuolo F, Celleno L, Ando S, Picci N, Calviello G and Palloza P 2004 Antioxidant effect of ferulic acid in isolated membranes and intact cells: synergistic interactions with alpha-tocopherol, beta-carotene and ascorbic acid.J. Agric. Food Chem.52 (8) pp 2411-2420.
12. 13.J Mishra, AK Dash, R Kumar ; Nanotechnology Challenges; Nanomedicine: Nanorobots International Research Journal of Pharmaceuticals, Volume,2 Issue 4 (2012)
13. Abramovič H. and Abraham N 2006 Effect of added rosemary extract on oxidative stability of Camelina sativa oil. Acta Agric. Slov. 87 (2) pp 255-261.
14. Kowalski R 2007 GC analysis of changes in the fatty acid composition of sunflower and olive oils heated with quercetin, caffeic acid, protocatechuic acid and butylated hydroxyaniosle. Acta Chromatogr. 18 pp 15-23.
15. Zolnik BS and Sadrich N 2009 Regulatory perspective on the importance of ADME assessment of nanoscale material containing drugs. Adv. Drug Deliv. Rev. 61 (6) pp 422-427.
16. Miyazaki K and Islam N 2007 Nanotechnology systems of innovation. An analysis of industry and academia research activities. Technovation 27 (11) pp 661-675.
17. D Saha, S Mandal, B Biswal, AK Dash, J Mishra: Anti diabetic activity of the bark of parkinsonia aculeata in streptozotocin induced diabetic rats. Artigo em Inglês | IMSEAR | ID: sea-161323,(2011)
18. Peiris PM, Bauer L, Toy R, Tran E, Pansky J, Doolittle E, Schmidt E, Hayden E, Mayer A, Keri RA and Griswold MA 2012 Enhanced delivery of chemotherapy to tumor using a multicomponent nanochain with radiofrequency tunable drug release. ACS Nano 6 (5) pp4157-4168.

19. Shakti Jaiswal, Alok Kumar Dash,*Jhansee Mishra. Development and characterization of a novel nano-liposomal formulation of famotidine-loaded nano-sized liposomal with biodegradable polymer. Bull. Env. Pharmacol. Life Sci., Vol 12[6] May 2023: 82-91.
20. Radovic-Moreno AF, Lu TK, Puscasu VA, Yoon CJ, Langer R, Farokhzad OC 2012 Surface charge-switching polymeric nanoparticles for bacterial cell wall-targeted delivery of antibiotics. ACS Nano 6 (5) pp 4279-4287.
21. Wong HL, Wu XY and Bendayan R 2012 Nanotechnology advances for the delivery of central nervous system therapeutics. Adv. Drug Deliv. Rev. 64 (7) pp 686-700.
22. Shakti Jaiswal, Alok Kumar Dash,,Jhansee Mishra. Development and characterization of a novel nano-liposomal formulation of famotidine-loaded nano-sized liposomal with biodegradable polymer. Bull. Env. Pharmacol. Life Sci., Vol 12[6] May 2023: 82-91
23. Sood R and Chopra DS 2017 Improved yield of green synthesized crystalline silver nanoparticles with potential antioxidant activity. Int. Res. J. Pharm. 8 (4) pp 4-17.onoids as antioxidants. J. Nat. Prod. 2000 63 (7) pp 1035-1042.
24. A.W. Bauer, W.M.M. Kirby, J.C. Serris, M. Turck, Am. J. Clin. Pathol. 45, 493–496 (1966)26. Akintola AO, Ayoola PB and Ibikunle GJ 2012 Antioxidant activity of two Nigerian green leafy vegetables. J. Pharmaceut. Biomed. Sci. 14 (15) pp 1-5.
25. DA Kumar, S Dharmendra, M Jhansee, N Shrikant: Development and characterization of chitosan nanoparticles loaded with amoxicillin; Int Res J Pharmacy, Volume – 2;(2011)
26. Tarusco TG, Barney DL and Exon TJ 2004 Content and profile of flavonoid and phenolic acid compounds in conjunction with antioxidant capacity for a variety of North West Vaccinium berriers. J. Agric. Food Chem. 52 (10) pp 3169-3176.
27. AK Dash, J Mishra ; Formulation and in vitro characterization of chitosannanoparticles loaded with ciprofloxacin hydrochloride; Der Pharmacia Lettre, Volume-5,Issue-4,126-131(2013)
28. Pieta PG 2000 Flavonoids as antioxidants. J. Nat. Prod. 2000 63 (7) pp 1035-1042.